Sloshing Effects in Half-Full Horizontal Cylindrical Vessels Under Longitudinal Excitation

S. Papaspyrou

D. Valougeorgis[1]
e-mail: diva@mie.uth.gr
Mem. ASME

S. A. Karamanos

Department of Mechanical and Industrial Engineering,
University of Thessaly,
Volos 38334, Greece

A mathematical model is developed for sloshing effects in half-full horizontal cylindrical vessels, under external excitation in the direction of the longitudinal vessel axis. In this geometry the problem is not separable. The velocity potential is expressed in a double series form, and after some mathematical manipulation the problem results in a series of systems of ordinary linear differential equations, one for each longitudinal mode. For the particular case of harmonic motion, a semi-analytical solution is possible. Keeping only the first two terms of the expansion in the transverse direction, an elegant formulation of remarkable accuracy is obtained. Hydrodynamic pressures and forces are calculated for harmonic excitation and for a real seismic motion event. Finally, the equivalence between the half-full horizontal cylinder and an "equivalent" rectangle is demonstrated.
[DOI: 10.1115/1.1668165]

1 Introduction

The linearized sloshing problem can be treated as an eigenvalue problem, representing free fluid vibrations inside a container, and provides the sloshing frequencies and modes. Under a specific external excitation it is converted into a transient problem, representing fluid motion within the moving container.

The sloshing solution depends strongly on the container shape. For nondeformable rectangular and vertical-cylindrical containers the sloshing problem for ideal fluids can be solved analytically, using separation of variables, [1], resulting in a set of uncoupled equations, one for each sloshing mode. In particular, the case of vertical cylindrical vessels has been extensively investigated since the late 1950s, mainly because of space vehicle applications, [2,3], as well as for determining the seismic response of liquid storage tanks, [4,5]. Based on this exact sloshing solution, other effects, such as tank wall deformation, [6,7], or soil-structure interaction, [7,8], can be considered in an approximate manner. The recent publication of Ibrahim et al. [9] offers a broad overview of sloshing dynamics with emphasis on vertical cylinders and rectangles.

Containers of different shape, such as horizontal cylinders or spheres have received much less attention. In these configurations exact analytical solutions may not be available and the use of numerical methods becomes necessary, in addition to experimental testing. Most of the work in horizontal cylinders is focused on the eigenvalue sloshing problem, towards the computation of sloshing frequencies and the corresponding modes in the transverse and longitudinal directions, [10–14]. Experimental measurements of sloshing frequencies in horizontal cylindrical vessels, were reported by McCarty and Stephens [15] and Kana [16]. The corresponding transient problem in the transverse direction has been studied in an early work by Budiansky [17], while, recently, Kobayashi et al. [18] reported experimental measurements for sloshing frequencies and hydrodynamic forces in both directions, which were compared with analytical results from equivalent rectangular containers.

Generally, sloshing analysis in horizontal cylindrical vessels filled up to an arbitrary height requires an approximate or numerical solution. However, for the particular case of half-full horizontal cylinders an analytical solution is possible. Evans and Linton [19] presented such a solution for the eigenvalue-sloshing problem (free fluid vibrations in a nondeformable container), expanding the velocity potential in terms of non-orthogonal bounded spatial functions.

The present work is aimed at calculating the response in half-full horizontal cylindrical containers under any form of longitudinal excitation, extending the analytical eigenvalue formulation of Evans and Linton [19]. In particular, the objective of the paper is the solution of externally induced liquid sloshing in half full cylinders under longitudinal excitation, through a semi-analytical manner, without implementing finite difference or finite element approximations. The present sloshing solution is divided in a "uniform motion" part, trivially obtained, and a part related to sloshing, representing the relative fluid motion within the container. Using a series expansion of the velocity potential, the problem reduces to a system of ordinary linear differential equations, which is solved numerically. For the case of harmonic excitation the formulation results in a system of algebraic equations yielding semi-analytical solutions of benchmark quality. Sloshing frequencies and modes, hydrodynamic pressures and the corresponding sloshing forces are computed in a simple and efficient manner. Dissipation effects are considered and their influence is examined. Furthermore, considering the first two terms of the series in the transverse direction, an elegant simplified formulation is obtained, which yields quite accurate results. The case of harmonic excitation and the response under a real seismic event are examined. The response of the half-full cylinder is compared with the response of an "equivalent" rectangular container, which has the same free-surface dimensions and contains the same amount of liquid. It is shown analytically and numerically that the equivalent rectangle can be used for approximating the response of the half-full cylinder.

2 Theoretical Formulation and Solution

2.1 Problem Statement. The fluid is contained in a horizontal cylindrical vessel of radius R and length L. In practical industrial applications, horizontal cylinders are very thick to resist

[1]To whom correspondence should be addressed.

Contributed by the Applied Mechanics Division of THE AMERICAN SOCIETY OF MECHANICAL ENGINEERS for publication in the ASME JOURNAL OF APPLIED MECHANICS. Manuscript received by the ASME Applied Mechanics Division, Mar. 3, 2003; final revision, July 15, 2003. Associate Editor: D. A. Siginer. Discussion on the paper should be addressed to the Editor, Prof. Robert M. McMeeking, Journal of Applied Mechanics, Department of Mechanical and Environmental Engineering University of California–Santa Barbara, Santa Barbara, CA 93106-5070, and will be accepted until four months after final publication of the paper itself in the ASME JOURNAL OF APPLIED MECHANICS.

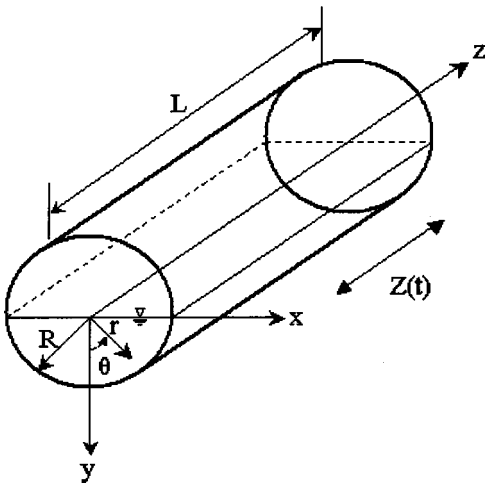

Fig. 1 Configuration of half-full horizontal cylindrical container

high levels of internal pressure and therefore, in our formulation, the vessel is assumed rigid (non deformable). Furthermore, the vessel is half full and undergoes an arbitrary motion in the direction of the longitudinal axis z with displacement $Z(t)$, as shown in Fig. 1. The amplitude of the external excitation and the resulting free surface elevation are assumed to be sufficiently small to allow linearization of the problem. It is assumed that the fluid inside the container is inviscid and the flow can be described by a velocity potential function $\Phi(r,\theta,z,t)$, which satisfies Laplace equation within the fluid volume:

$$\nabla^2\Phi=\frac{1}{r}\frac{\partial}{\partial r}\left(r\frac{\partial\Phi}{\partial r}\right)+\frac{1}{r^2}\frac{\partial^2\Phi}{\partial\theta^2}+\frac{\partial^2\Phi}{\partial z^2}=0,$$

$$r<R,\ -\pi/2<\theta<\pi/2,\ 0<z<L. \tag{1}$$

The velocity potential is subjected to the linearized dynamic and kinematic free-surface conditions

$$\frac{\partial\Phi}{\partial t}-g\,\eta=0,\quad \text{at } \theta=\pm\pi/2,\ r<R,\ 0<z<L \tag{2}$$

and

$$\pm\frac{1}{r}\frac{\partial\Phi}{\partial\theta}+\frac{\partial\eta}{\partial t}=0,\quad \text{at } \theta=\pm\pi/2,\ r<R,\ 0<z<L, \tag{3}$$

respectively, where g is the gravitational constant and $\eta=\eta(r,z,t)$ is the free-surface elevation. Combination of boundary conditions (2) and (3) leads to the mixed boundary condition

$$\frac{\partial^2\Phi}{\partial t^2}\pm\frac{1}{r}\frac{\partial\Phi}{\partial\theta}=0,\quad \text{at } \theta=\pm\pi/2,\ r<R,\ 0<z<L. \tag{4}$$

Moreover, Φ should satisfy the kinematic conditions at the walls of the rigid container

$$\frac{\partial\Phi}{\partial r}=0,\quad \text{at } r=R,\ -\pi/2<\theta<\pi/2,\ 0<z<L \tag{5}$$

and

$$\frac{\partial\Phi}{\partial z}=\dot{Z}(t),\quad \text{at } z=0,\ L,\ -\pi/2<\theta<\pi/2,\ 0<r<R. \tag{6}$$

Subsequently, Φ is decomposed in two parts

$$\Phi(r,\theta,z,t)=f(z,t)+\varphi(r,\theta,z,t) \tag{7}$$

where $f(z,t)$ and $\varphi(r,\theta,z,t)$ are the "uniform motion" velocity potential and the potential related to sloshing, respectively. The velocity potential f corresponds to a "rigid body" motion of the fluid, which follows exactly the motion of the external excitation source, and satisfies the Laplace equation and the nonhomogeneous part of the kinematic conditions (6) at $z=0$ and $z=L$. Thus the solution of the "uniform motion" is antisymmetric with respect to $z=L/2$ and it is trivially obtained as

$$f(z,t)=\dot{Z}(t)\left(z-\frac{L}{2}\right). \tag{8}$$

Then the velocity potential φ, which represents the relative motion of the fluid particles within the container due to sloshing, should satisfy the Laplace equation within the fluid region and the following boundary conditions:

$$\frac{\partial^2\varphi}{\partial t^2}\pm\frac{g}{r}\frac{\partial\varphi}{\partial\theta}=-\frac{\partial^2 f}{\partial t^2},\quad \text{at } \theta=\pm\pi/2,\ r<R,\ 0<z<L \tag{9}$$

$$\frac{\partial\varphi}{\partial r}=0,\quad \text{at } r=R,\ -\pi/2<\theta<\pi/2,\ 0<z<L \tag{10}$$

and

$$\frac{\partial\varphi}{\partial z}=0,\quad \text{at } z=0,\ L,\ -\pi/2<\theta<\pi/2,\ 0<r<R. \tag{11}$$

It is noted that the boundary value problem stated above for the cylinder of semicircular cross section cannot be solved trivially by separation of variables.

2.2 Solution for the Potential Related to Sloshing. The solution of the problem related to sloshing contains certain characteristics. Due to the nature of the external excitation and the symmetry of the vessel geometry with respect to planes $z=L/2$ and $\theta=0$, the above expression is anti-symmetric in terms of z (longitudinal direction) and symmetric with respect to the $\theta=0$ plane. Thus a general solution for the unknown function φ satisfying the Laplace equation is considered in a series form as

$$\varphi(r,\theta,z,t)=\sum_{p=1,3,5}^{\infty}\sum_{n=0}^{\infty}\dot{q}_n^p(t)[I_n(k_pr)\cos(n\theta)]\cos(k_pz),$$

$$r<R,\ -\pi/2<\theta<\pi/2,\ 0<z<L \tag{12}$$

where $q_n^p(t)$ are unknown arbitrary time functions and $I_n(x)$ are the modified Bessel functions of order n. The boundary conditions (11) at $z=0$ and $z=L$ are satisfied provided that $k_p=p\pi/L$, $p=1,3,5,\ldots$ The expression of φ is rewritten in the form, [19],

$$\varphi(r,\theta,z,t)=\sum_{p=1,3,5}^{\infty}\sum_{n=0}^{\infty}\{\dot{q}_{2n}^p(t)\cos(2n\theta)I_{2n}(k_pr)+\dot{q}_{2n+1}^p(t)\cos[(2n+1)\theta]I_{2n+1}(k_pr)\}\cos(k_pz) \tag{13}$$

separating odd and even terms of the series in the transverse direction.

Substituting the above expression for φ into boundary condition (10) and applying the integral operator $\int_0^{\pi/2}\cdots\cos(2m\theta)d\theta$, $m=0,1,2\ldots$, the following relations between the even and odd unknown time functions are obtained:

$$\dot{q}_0^p(t)=-\frac{1}{\pi I_0'(k_pR)}\sum_{m=0}^{\infty}\frac{(-1)^m}{m+1/2}I_{2m+1}'(k_pR)\dot{q}_{2m+1}^p(t),$$

$$p=1,3,5,\ldots \tag{14}$$

and

$$\dot{q}^p_{2n}(t) = -\frac{1}{\pi I'_{2n}(k_pR)}\sum_{m=0}^{\infty}\left(\frac{(-1)^{m-n}}{m-n+1/2} + \frac{(-1)^{m+n}}{m+n+1/2}\right) I'_{2m+1}(k_pR)\dot{q}^p_{2m+1}(t),$$

$$n>0,\ \ p=1,3,\ldots \tag{15}$$

where $I'(x)$ denotes the derivative of the modified Bessel function with respect to x. Next substituting Eqs. (8) and (13) for $f(z,t)$ and $\varphi(r,\theta,z,t)$ respectively into boundary condition (9) yields

$$\sum_{p=1,3,5}^{\infty}\sum_{n=0}^{\infty}(-1)^n\left[\ddot{q}^p_{2n}(t)I_{2n}(k_pr) - q^p_{2n+1}(2n+1)\frac{g}{r}I_{2n+1}(k_pr)\right]\cos(k_pz) = -\left(z-\frac{L}{2}\right)\ddot{Z}(t). \tag{16}$$

Applying the integral operator $\int_0^L\cdots\cos(k_Sz)dz$, $s=1,3,5,\ldots$, the double sum of Eq. (16) is converted into a system of equations

$$\sum_{n=0}^{\infty}(-1)^n\left[\ddot{q}^p_{2n}(t)I_{2n}(k_pr) - q^p_{2n+1}(2n+1)\frac{g}{r}I_{2n+1}(k_pr)\right] = \frac{4}{Lk_p^2}\ddot{Z}(t),\quad p=1,3,5\ldots. \tag{17}$$

Then, using the identity, [20],

$$(2n+1)I_{2n+1}(x) = \frac{x}{2}[I_{2n}(x) - I_{2n+2}(x)] \tag{18}$$

one obtains

$$\sum_{n=0}^{\infty}(-1)^n\left[\ddot{q}^p_{2n}(t) - q^p_{2n+1}(t)\frac{k_pg}{2} - q^p_{2n-1}(t)\frac{k_pg}{2}\right]I_{2n}(k_pr) = \frac{4}{Lk_p^2}\ddot{Z}(t), \tag{19}$$

with $q_{-1}=0$. Subsequently, implementing the following expansion, [20],

$$1 = I_0(x) - 2I_2(x) + 2I_4(x) - 2I_6(x) + 2I_8(x)\ldots \tag{20}$$

and equating terms of equal order in n, the following expressions are obtained:

$$\ddot{q}^p_0(t) - \frac{k_pg}{2}q^p_1(t) = \frac{4}{k_p^2L}\ddot{Z}(t),\quad p=1,3,5,\ldots \tag{21}$$

and

$$\ddot{q}^p_{2n}(t) - \frac{k_pg}{2}q^p_{2n+1}(t) - \frac{k_pg}{2}q^p_{2n-1}(t) = \frac{8}{k_p^2L}\ddot{Z}(t),$$

$$n>0,\ \ p=1,3,5,\ldots. \tag{22}$$

Finally by substituting Eqs. (14) and (15) into Eqs. (21) and (22), respectively, the following infinite system of second-order ordinary differential equations is deduced for each mode p:

$$[\mathbf{M}^p]\{\ddot{q}^p\} + [\mathbf{K}^p]\{q^p\} = -\{\gamma^p\}\ddot{Z}\quad p=1,3,5,\ldots \tag{23}$$

where $[\mathbf{M}^p]$ and $[\mathbf{K}^p]$ are square matrices, $\{\gamma^p\}$ is a vector, with elements

$$M^p_{0m} = \left(\frac{(-1)^m}{m+1/2}\right)\frac{I'_{2m+1}(k_pR)}{I'_0(k_pR)},\quad m=0,1,2,\ldots,\ \ p=1,3,5,\ldots \tag{24}$$

$$M^p_{nm} = \left(\frac{(-1)^{m-n}}{m-n+1/2} + \frac{(-1)^{m+n}}{m+n+1/2}\right)\frac{I'_{2m+1}(k_pR)}{I'_{2n}(k_pR)},$$

$$n>0,\ \ m=0,1,2,\ldots,\ \ p=1,3,5,\ldots \tag{25}$$

$$[\mathbf{K}^p] = \frac{k_p\pi}{2}g\begin{bmatrix} 1 & 0 & \cdots & \cdots & \cdots & 0 & \cdots \\ 1 & 1 & 0 & \cdots & \cdots & 0 & \cdots \\ \cdots & \cdots & \cdots & \cdots & \cdots & \cdots & \cdots \\ 0 & \cdots & 0 & 1 & 1 & 0 & \cdots \\ 0 & \cdots & \cdots & 0 & 1 & 1 & \cdots \\ \vdots & \vdots & \vdots & \vdots & \vdots & \vdots & \ddots \end{bmatrix},$$

$$p=1,3,5,\ldots \tag{26}$$

$$\gamma^p_0 = \frac{4\pi}{k_p^2L},\quad \gamma^p_n = \frac{8\pi}{k_p^2L},\quad n>0,\ \ p=1,3,5,\ldots \tag{27}$$

and $\{q^p\}$ is the unknown vector with components $q^p_{2m+1}(t)$, $m=0,1,2,\ldots$. Solution of vector Eq. (23) is performed through a typical time-marching numerical scheme, and leads to the calculation of functions $q^p_{2m+1}(t)$ and their derivatives. For computational purposes a truncated series in Eq. (13) is considered ($n<N$, where N is the truncation size), and a truncated system of ordinary differential equations is obtained, which is solved in terms of $q^p_{2n+1}(t)$. Subsequently, Eqs. (14) and (15) are used to determine the even functions $q^p_{2n}(t)$, so that the potential φ associated with sloshing is completely defined.

The elevation of the free surface is obtained by integrating the kinematic boundary condition (3) with respect to time:

$$\eta(r,z,t) = \sum_{p=1,3,5}^{\infty}\sum_{n=0}^{\infty}q^p_{2n+1}(t)\frac{(2n+1)}{r}I_{2n+1}(k_pr)\cos(k_pz). \tag{28}$$

2.3 Energy Dissipation. To account for dissipation effects, a damping term proportional to the first derivative of the generalized coordinates is introduced in Eqs. (23),

$$[\mathbf{M}^p]\{\ddot{q}^p\} + [\mathbf{C}^p]\{\dot{q}^p\} + [\mathbf{K}^p]\{q^p\} = -\{\gamma^p\}\ddot{Z}, \tag{29}$$

where $[\mathbf{C}^p]$ is a square matrix, considered in the form of a Rayleigh damping matrix

$$[\mathbf{C}^p] = \alpha_0[\mathbf{M}^p] + \alpha_1[\mathbf{K}^p] \tag{30}$$

where α_0 and α_1 are constants.

It is interesting to note that in previous works, [21,22], a different formulation was proposed to model damped systems, which enables the use of potential theory and introduces a damping term proportional to the potential related to sloshing in the dynamic boundary condition as

$$\frac{\partial\Phi}{\partial t} + \nu\varphi - g\eta = 0,\quad \text{at}\ \ \theta = \pm\pi/2,\ \ r<R,\ \ 0<z<L. \tag{31}$$

The extra term represents a force, which opposes particle velocity, and the proportionality constant ν is a viscosity coefficient. Equation (31) leads to the following mixed boundary condition at the free surface

$$\frac{\partial^2\Phi}{\partial t^2} + \nu\frac{\partial\varphi}{\partial t} \pm \frac{g}{r}\frac{\partial\Phi}{\partial\theta} = 0,\quad \text{at}\ \ \theta = \pm\pi/2,\ \ r<R,\ \ 0<z<L. \tag{32}$$

If boundary condition (32), instead of (4), is implemented in the formulation, it yields a system of ordinary differential equations identical to that of Eq. (29), with $[\mathbf{C}^p] = \nu[\mathbf{M}^p]$, a special form of Raleigh damping.

2.4 Hydrodynamic Pressures and Forces. Once the velocity potential φ associated with sloshing is calculated, the hydrodynamic pressure at any location can be computed from the linearized Bernoulli equation

$$P(r,\theta,z,t)=-\rho\frac{\partial\Phi}{\partial t}=-\rho\frac{\partial f}{\partial t}-\rho\frac{\partial\varphi}{\partial t}. \tag{33}$$

On the right-hand side of Eq. (33) the first term refers to the uniform motion, while the second term refers to sloshing effects. The pressure associated with sloshing at $z=L$ is

$$P_{s,z=L}=\rho\sum_{p=1,3,5}^{\infty}\sum_{n=0,}^{\infty}\ddot{q}_n^p I_n(k_p r)\cos(n\theta). \tag{34}$$

The total horizontal force acting on the container is obtained by an appropriate integration of the pressure as

$$F=\int_A P(r,\theta,z,t)(\mathbf{e}_z\cdot\mathbf{n})dA \tag{35}$$

where A is the area of the two "wet" semicircular ends of the container ($z=0$, $z=L$), $\mathbf{e}_z$ is the unit vector in the z direction (Fig. 1), and $\mathbf{n}$ the outer unit vector normal to A. From Eqs. (33) and (35), the total force F can be also expressed as the sum of the "uniform motion" force F_U and the force associated with sloshing F_S

$$F_U=-\rho\int_A\frac{\partial f}{\partial t}(\mathbf{e}_z\cdot\mathbf{n})dA \quad \text{and} \quad F_S=-\rho\int_A\frac{\partial\varphi}{\partial t}(\mathbf{e}_z\cdot\mathbf{n})dA, \tag{36}$$

respectively, so that $F=F_U+F_S$. The uniform motion force is readily calculated as

$$F_U=-\left(\frac{1}{2}\pi\rho R^2 L\right)\ddot{Z}=-M_L\ddot{Z} \tag{37}$$

where

$$M_L=\frac{1}{2}\pi\rho R^2 L \tag{38}$$

is the total liquid mass. The force related to sloshing at $z=L$ is calculated by integrating the pressure on the end section $z=L$

$$F_{SL}=M_L\sum_{p=1,3,5,\ldots}^{\infty}\left[2S_{0,1}^p\frac{\ddot{q}_0^p}{L}+\sum_{n=1,3,5,\ldots}^{\infty}(-1)^{(n-1)/2}\left(\frac{4}{n\pi}\right)S_{n,1}^p\frac{\ddot{q}_n^p}{L}\right] \tag{39}$$

where

$$S_{m,k}^p=\int_0^1\xi^k I_m(k_p R\xi)d\xi. \tag{40}$$

The total force associated with sloshing F_S is equal to twice the value of force F_{SL}, due to the antisymmetry of the solution. It is interesting to note that from the series expansion in the transverse direction (i.e., summation with respect to n), all odd terms ($n=1,3,5\ldots$) contribute to the sloshing force, whereas from the even terms only the first term ($n=0$) contributes.

3 Simplified Solution and Mechanical Model

It is possible to develop a simplified version of the above formulation considering only the first two terms of the series expansion of the potential φ in the transverse direction (truncation size $N=0$ in Eq. (13)). This yields elegant expressions of very good accuracy for frequencies, pressures and forces, and motivates the development of an equivalent mechanical model.

3.1 Simplified Sloshing Solution. Assuming that the potential related to sloshing φ is equal to

$$\varphi=\sum_{p=1,3,5}^{\infty}[\dot{q}_0^p I_0(k_p r)+\dot{q}_1^p\cos\theta I_1(k_p r)]\cos(k_p z) \tag{41}$$

and applying the boundary conditions, the following equations are obtained

$$\dot{q}_0^p=-\left[\frac{2}{\pi}\frac{I_1'(k_p R)}{I_0'(k_p R)}\right]\dot{q}_1^p=-B_p\dot{q}_1^p \quad p=1,3,5,\ldots \tag{42}$$

and

$$\ddot{q}_1^p+\frac{1}{2}\left(\frac{gk_p}{B_p}\right)q_1^p=-\frac{4L}{p^2\pi^2 B_p}\ddot{Z}, \tag{43}$$

which are analogous to Eqs. (14) and (23), respectively. To account for dissipation effects, a damping term may be introduced in each equation, proportional to the first derivative of the unknown time function:

$$\ddot{q}_1^p+\alpha_p\dot{q}_1^p+\frac{1}{2}\left(\frac{gk_p}{B_p}\right)q_1^p=-\frac{4L}{p^2\pi^2 B_p}\ddot{Z} \tag{44}$$

which is an equation analogous to Eq. (29), and α_p is constant. This equation can also be written in the form of a linear oscillator equation

$$\ddot{q}_1^p+2\xi_p\omega_{sp}\dot{q}_1^p+\omega_{sp}^2 q_1^p=-\left(\frac{2L}{p^2\pi}\right)\frac{I_0'(k_p R)}{I_1'(k_p R)}\ddot{Z} \quad p=1,3,5,\ldots \tag{45}$$

where

$$\omega_{sp}^2=\frac{g\pi k_p}{4}\frac{I_0'(k_p R)}{I_1'(k_p R)} \tag{46}$$

is the circular (undamped) sloshing frequency corresponding to the pth mode obtained with the simplified methodology and

$$\xi_p=\alpha_p/2\omega_{sp} \tag{47}$$

is the corresponding damping ratio. Equation (47) can be employed to estimate the value of α_p, if the damping ratio ξ_p for a certain mode p is somehow estimated (e.g., experimentally). Furthermore, the ω_{sp} value is an approximation of the first sloshing frequency of the pth mode, since only the first two terms of the series expansion in the transverse direction are employed, and can be expressed in the following nondimensional form:

$$\frac{\omega_{sp}^2 R}{g}=\frac{\pi}{4}k_p R\frac{I_0'(k_p R)}{I_1'(k_p R)} \tag{48}$$

which indicates sloshing frequencies depend on the container aspect ratio (L/R).

The hydrodynamic pressure and force associated with sloshing on the wall at $z=L$ are

$$P_{s,z=L}=\rho\sum_{p=1,3,5}^{\infty}[-B_p I_0(k_p r)+\cos\theta I_1(k_p r)]\ddot{q}_1^p \tag{49}$$

and

$$F_{SL}=-M_L\sum_{p=1,3,5}^{\infty}\frac{1}{L}\left[2B_p S_{0,1}^p-\frac{4}{\pi}S_{1,1}^p\right]\ddot{q}_1^p, \tag{50}$$

respectively, where $S_{m,k}^p$ is defined in Eq. (40) and B_p in Eq. (42). The force F_{SL} is applied at a certain location on the symmetry axis $x=0$ of the end section $z=L$ (Fig. 1). Then the moment $\mathcal{M}_{SL}$ of force F_{SL} about the x-axis is

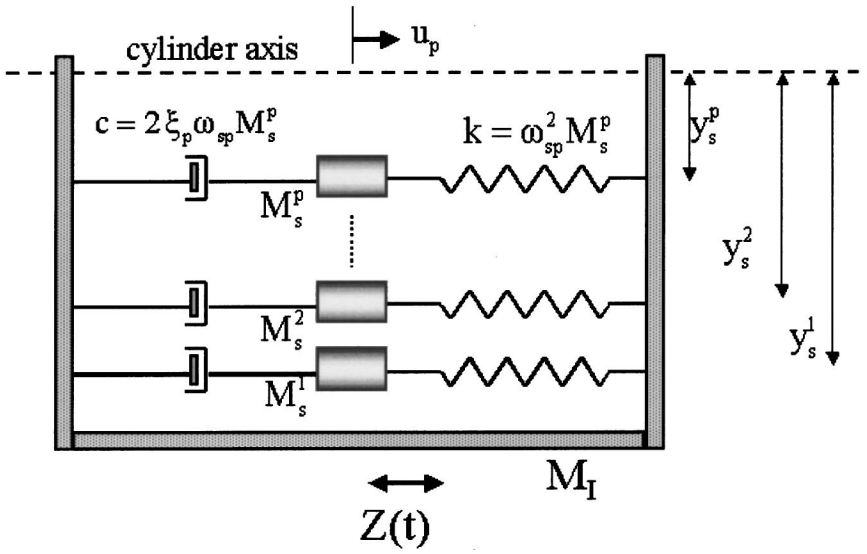

Fig. 2 Mechanical model approximating the sloshing response of a half-full cylindrical container

$$\mathcal{M}_{SL} = \int_{A(z=L)} y P_{s,z=L} dA = \int_{-\pi/2}^{\pi/2} \int_0^R P_{s,z=L} r^2 \cos\theta dr d\theta$$

$$= -M_L R \sum_{p=1,3,5}^{\infty} \frac{1}{L} \left[\frac{4B_p}{\pi} S_{0,2}^p - S_{1,2}^p \right] \ddot{q}_1^p \tag{51}$$

and the distance y_s of force F_{SL} from the cross-section center is equal to the ratio $\mathcal{M}_{SL}/F_{SL}$. The entire force associated with sloshing F_S is the sum of the forces at $z=0$ and $z=L$ and the total force F is the sum of F_S and F_U where the uniform motion force F_U is given by Eq. (37).

3.2 Equivalent Mechanical Model. The above simplified solution motivates the development of an equivalent mechanical model, which approximates the liquid-container response. Introducing a new variable $x_p(t)$ for each mode p,

$$x_p = \left(\frac{p^2 \pi}{2L} \right) \frac{I_1'(k_p R)}{I_0'(k_p R)} q_1^p \tag{52}$$

the corresponding equation of motion becomes

$$\ddot{x}_p + 2\xi_P \omega_{SP} \dot{x}_p + \omega_{SP}^2 x_p = -\ddot{Z}. \tag{53}$$

Furthermore, the entire force associated with sloshing becomes

$$F_S = \sum_{p=1,3,5}^{\infty} F_S^P = -\sum_{p=1,3,5}^{\infty} M_S^P \ddot{x}_p \tag{54}$$

where

$$M_S^p = \left[\frac{16}{p^2 \pi^2} \left(S_{0,1}^p - \frac{2}{\pi B_p} S_{1,1}^P \right) \right] M_L \tag{55}$$

and

$$F_S^P = -M_S^P \ddot{x}_p \tag{56}$$

is the sloshing force corresponding to mode p. In the above equation, M_S^P expresses the part of liquid mass associated with sloshing motion, which refers to mode p. Equations (53) and (54) corresponds to a series of oscillators, one for each longitudinal mode p. Setting

$$u_p = x_p + Z, \tag{57}$$

it is straightforward to rewrite Eqs. (53) and (54) in the form

$$M_S^p \ddot{u}_p + 2\xi_p \omega_{sp} M_S^p (\dot{u}_p - \dot{Z}) + \omega_{sp}^2 M_S^p (u_p - Z) = 0 \tag{58}$$

and

$$F = -\sum_{p=1,3,5,\ldots}^{\infty} M_S^p \ddot{u}_p - M_I \ddot{Z} \tag{59}$$

where

$$M_I = M_L - \sum_{p=1,3,5,\ldots}^{\infty} M_S^p. \tag{60}$$

Based on Eqs. (58) and (59), the liquid-container system is simulated through a series of linear oscillators as shown in Fig. 2. In this model, Z represents the external source motion, and u_p expresses the motion of the liquid mass associated with sloshing mode p. Furthermore, the total liquid mass M_L is split in a part M_I, which follows the motion of $Z(t)$, expressing the so-called "impulsive" motion, and a series of masses M_S^p ($p=1,3,5,\ldots$), which correspond to $u_p(t)$, expressing the so-called "convective" (or "sloshing") motion, [3,4]. The position y_S^p of each oscillator on the y-axis is calculated through their moments about the x-axis. It is readily obtained that

$$\frac{y_S^p}{R} = \left[\frac{S_{1,2}^P - \dfrac{4B_p}{\pi} S_{0,2}^p}{\dfrac{4}{\pi} S_{1,1}^P - 2B_p S_{0,1}^p} \right] \tag{61}$$

indicating that y_S^p depends on the aspect ratio (L/R) of the container. As an example, for $L/R = 3\pi$, the y_S^p/R values for oscillators corresponding to modes $p=1$, $p=3$, and $p=5$ are 0.419, 0.379, and 0.296, respectively.

4 Solution for Harmonic Excitation

The mathematical formulation for arbitrary excitation is significantly simplified when the rigid container undergoes a harmonic motion

$$\dot{Z}(t) = U e^{-i\omega t}, \tag{62}$$

where U is the velocity amplitude, and ω is the angular frequency of the external excitation source. Assuming steady-state conditions, the velocity potentials become

$$f(z,t)=\left(z-\frac{L}{2}\right)Ue^{-i\omega t} \tag{63}$$

and

$$\dot{q}_n^p(t)=a_n^p e^{-i\omega t} \tag{64}$$

so that

$$\varphi(r,\theta,z,t)=\sum_{p=1,3,5}^{\infty}\sum_{n=0}^{\infty}\{a_{2n}^p\cos(2n\theta)I_{2n}(k_pr) + a_{2n+1}^p\cos[(2n+1)\theta]I_{2n+1}(k_pr)\}\cos(k_pz)e^{-i\omega t} \tag{65}$$

an equation analogous to Eq. (13). Applying the boundary conditions, the following infinite system of linear algebraic equations is obtained

$$(-\omega^2[\mathbf{M}^p]+[\mathbf{K}^p])\{a^p\}=\omega^2U\{\gamma^p\},\quad p=1,3,5,\ldots. \tag{66}$$

In the above system, the square matrix $[\mathbf{M}^p]$, the diagonal matrix $[\mathbf{K}^p]$ and the vector $\{\gamma^p\}$ are given by Eqs. (24)–(27) and $\{a^p\}$ is the unknown vector with components a_{2n+1}^p, $n=0,1,2,\ldots$. Similarly, the response of the damped system is obtained through the solution of the algebraic system

$$(-\omega^2[\mathbf{M}^p]-i\omega[\mathbf{C}^p]+[\mathbf{K}^p])\{a^p\}=\omega^2U\{\gamma^p\} \tag{67}$$

where the matrix $[\mathbf{C}^p]$ is given by Eq. (30).

Subsequently, the hydrodynamic pressures and the force acting on the container can be computed from Eqs. (33) and (35), respectively. It is interesting to note that in the case of harmonic excitation the present approach may be considered as semi-analytical since the only computational work required is the solution of a truncated linear algebraic system. If $U=0$, Eqs. (66) reduce to a homogeneous system, identical to the one obtained in [19].

An estimate of the externally induced sloshing effects on the response can be obtained from the added mass coefficient, [22], for each longitudinal mode p, defined as

$$C_a^p=\mathrm{Re}\left[\frac{F_S^p}{F_U}\right]. \tag{68}$$

On the other hand, the dimensionless damping coefficient

$$C_\nu^p=\mathrm{Im}\left[\frac{F_S^p}{F_U}\right] \tag{69}$$

provides a measure of dissipation effects when damping is included, [22]. In the above expressions, Re[ ] and Im[ ] denote the real and the imaginary part of the F_s^p/F_U ratio, respectively.

It is possible to obtain an elegant closed-form analytical solution for harmonic excitation, if the velocity potential φ is approximated only with the first two terms of the series expansion in the transverse direction ($n=N=0$ in Eq. (65)). In such a case, φ becomes

$$\varphi(r,\theta,z,t)=\sum_{p=1,3,5}^{\infty}\frac{4U}{k_p^2L}\frac{\omega^2}{\omega_{sp}^2-\omega^2}\left[-I_0(k_pr)+\frac{1}{B_p}\cos\theta I_1(k_pr)\right]\cos(k_pz)e^{-i\omega t} \tag{70}$$

and the force F_s^p corresponding to sloshing mode p is

$$F_s^p=i\omega U\rho\frac{4R^2L}{p^2\pi^2}\frac{\omega^2}{\omega_{sp}^2-\omega^2}\left[S_{0,1}^p-\frac{I_0'(k_pR)}{I_1'(k_pR)}S_{1,1}^p\right]e^{-i\omega t}. \tag{71}$$

Finally, the added mass coefficient and the dimensionless damping coefficient for mode p are

$$C_a^p=\frac{16}{p^2\pi^2}\left(S_{0,1}^p-\frac{I_0'(k_pR)}{I_1'(k_pR)}S_{1,1}^p\right)\frac{\lambda^2(1-\lambda^2)}{(1-\lambda^2)^2+(2\xi_{sp}\lambda)^2} \tag{72}$$

and

$$C_\nu^p=\frac{16}{p^2\pi^2}\left(S_{0,1}^p-\frac{I_0'(k_pR)}{I_1'(k_pR)}S_{1,1}^p\right)\frac{2\xi_{sp}\lambda^3}{(1-\lambda^2)^2+(2\xi_{sp}\lambda)^2}, \tag{73}$$

respectively, where $\lambda=\omega/\omega_{sp}$ is the ratio of the external frequency over the natural frequency of the oscillator.

5 Numerical Results and Discussion

The numerical results presented in this section are based on the solution of the truncated systems (67) and (29) for harmonic and arbitrary excitation, respectively. The results for the eigenvalue problem are based on the solution of system (67) with $U=0$.

5.1 Sloshing Frequencies, Modes, and Masses. The eigenvalue problem is considered first, assuming no external excitation. The convergence rate and the expected accuracy of the eigenvalues are demonstrated numerically, increasing the value of truncation size N ($n<N$ in Eq. (13)). In Figs. 3(a) and 3(b) the variation of the first three eigenvalues ω_1^p, ω_2^p, and ω_3^p, for the first two longitudinal modes ($p=1$ and $p=3$) in terms of the truncation size N for the case of zero dissipation is presented with $L/R=\pi$. In Fig. 3(c) the effect of the cylinder aspect ratio L/R is shown, presenting similar results for $L/R=3\pi$. From the numerical point-of-view, the results indicate that the convergence rate is quite rapid, and that faster convergence is obtained in lower sloshing frequencies. The required truncation size N to obtain accurate results up to three significant figures for the eigenvalues ω_1^p, ω_2^p, and ω_3^p in Fig. 3 is $N=3$, $N=6$, and $N=10$, respectively. The values of the computed eigenfrequencies are in very good agreement with experimental results, [16,17], and analytical predictions, [19].

It should be underlined that due to the nonorthogonality of the corresponding spatial functions in the transverse direction, the sloshing frequency values ω_j^p, $j=1,2,\ldots$, in the present formulation depend on the truncation size of the series expansion N. It is also important to note that for each longitudinal mode p, more than one eigenvalues are obtained, depending upon the truncation size N. On the other hand, when a series solution approach is applied in rectangles, mutually orthogonal functions are employed, and the corresponding sloshing modes are uncoupled yielding one eigenvalue for each longitudinal mode (see the Appendix). It is clarified that the sloshing problem in a longitudinally excited horizontal cylinder is a three-dimensional problem whereas the corresponding problem in a rectangle is reduced in a two-dimensional problem. In Fig. 4, the converged value ω_1^p of the first frequency for each mode p ($p=1,3,5,7$) is compared with the corresponding sloshing frequency ω_{rec}^p of an ''equivalent'' rectangular container (Eq. ($A6$)). The ''equivalent'' container has the same free surface dimensions $L\times 2R$, and a depth h equal to $\pi R/4$ so that it contains the same liquid volume with the horizontal cylinder. The very good comparison between ω_{rec}^p and ω_1^p is a good indication that this rectangular container can be used for approximating sloshing effects in horizontal cylinders, in practical engineering applications.

Figure 4 also shows that the ω_{sp} values ($p=1,3,5,7$), obtained from the simplified methodology (Eq. (48)), are fairly close to the corresponding values ω_1^p and ω_{rec}^p. Therefore, ω_{sp} offer a reasonable estimate of the converged value ω_1^p for each longitudinal mode p. Note that the ω_1^p and ω_{sp} values almost coincide for relatively long cylinders ($L/R\geqslant 3\pi$). Mathematically, the equivalence of ω_{rec}^p and ω_{sp} values for long rectangles and cylinders is

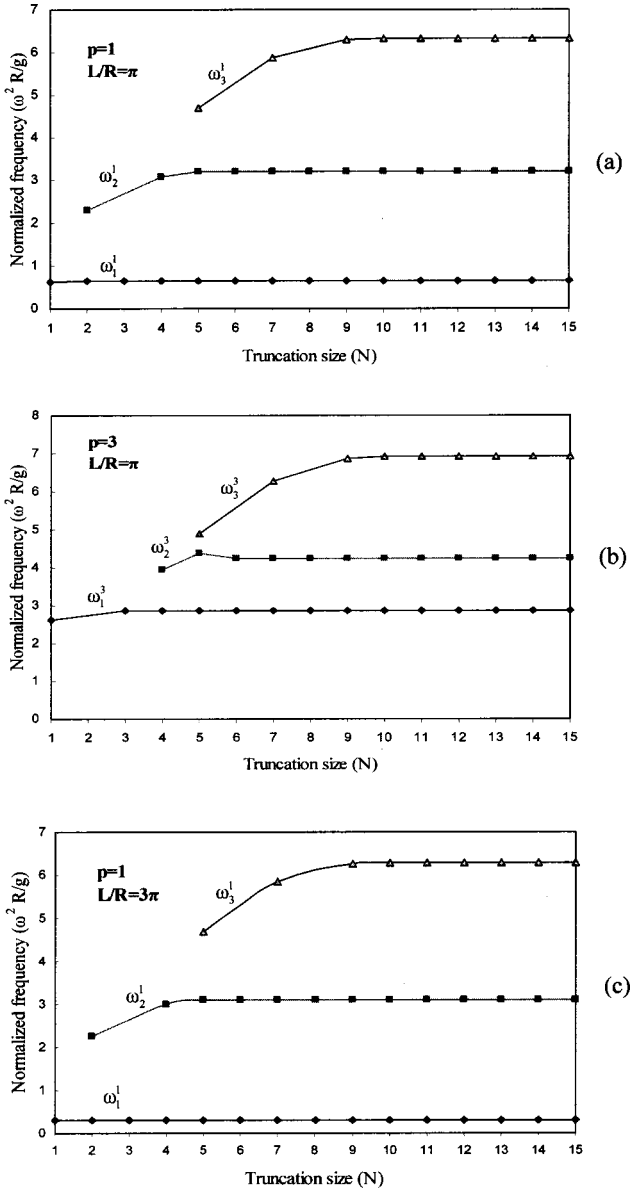

Fig. 3 Variation of sloshing frequencies with respect to the truncation size *N*

readily proved by considering the limit of expressions (46) and (*A*6) as $h/L \to 0$ and $R/L \to 0$, respectively. More specifically,

$$\lim_{R/L \to 0} \frac{\omega_{sp}^2 R}{g} = (k_p R)^2 \frac{\pi}{4} \tag{74}$$

and

$$\lim_{h/L \to 0} \frac{(\omega_{\text{rec}}^p)^2 R}{g} = (k_p R)^2 \frac{h}{R}. \tag{75}$$

The two limits are equal for $h = \pi R/4$, which is exactly the depth of the ''equivalent'' rectangular container.

In Fig. 5 sloshing modes corresponding to frequencies ω_1^1, ω_2^1, ω_3^1 $(p=1)$ are depicted in terms of their free-surface elevation. Note that the mode corresponding to ω_1^1 is quite similar to the mode corresponding to ω_{rec}^1 of an ''equivalent'' rectangular container. In Fig. 5(*a*), the slight curvature of the free surface in the transverse direction offers a reasonable explanation for the very small difference between the values of ω_1^1 and ω_{rec}^1.

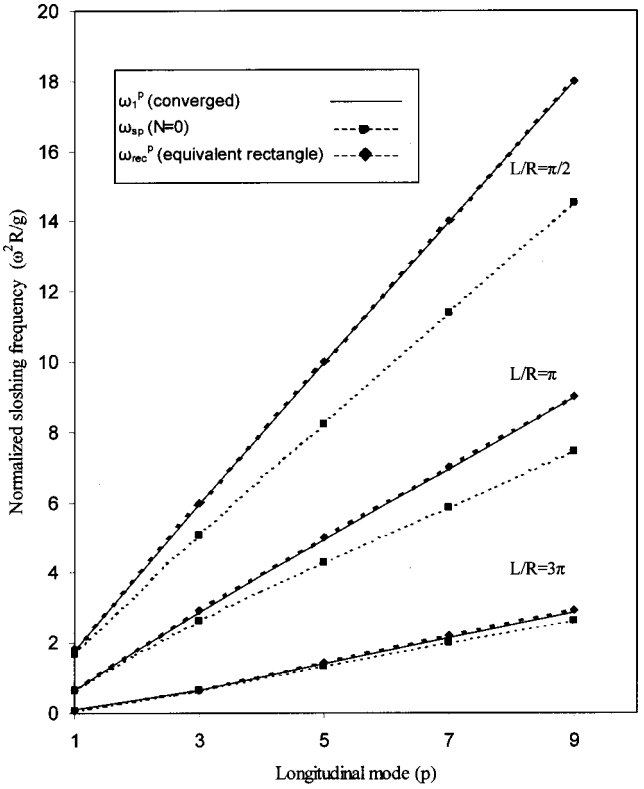

Fig. 4 Dominant eigenvalues for each longitudinal mode *p* and various aspect ratios of the container (*L*/*R*)

5.2 Hydrodynamic Forces Under Harmonic Longitudinal Excitation. Results under harmonic excitation are shown in terms of the added mass coefficient C_a^p and the dimensionless damping coefficient C_v^p. The C_a^p and C_v^p values $(p=1)$ are plotted in Figs. 6(*a*) and 6(*b*), respectively, in terms of the normalized external excitation frequency $(\omega^2 R/g)$. Damping is considered in the form of Eq. (30) with α_0 equal to 0, 0.25 and 0.50 and $\alpha_1 = 0$. It should be noted that the C_a^p and C_v^p values are ''converged'' values in the sense that they are obtained with an adequate truncation $n < N$ of Eq. (65). Figure 6(*a*) shows that for the case of zero damping, the response is characterized by large increases in the C_a^p value in the vicinity of resonant frequencies. A larger value of truncation size *N* is required for convergence close to the resonant frequencies. There is a sign reversal in C_a^p at each resonant frequency. When $C_a^p < 0$ the sloshing force F_s^p is out-of-phase with the container's displacement (i.e., the ''uniform motion'' force F_U) resulting in a reduction of the total force amplitude. The extreme values of C_a^p close to the resonant frequencies are significantly reduced when damping is present, and the resonant effect of the higher natural frequencies almost disappears. The large values of C_a^p for a wide range of excitation frequencies indicate the significant effects of hydrodynamic sloshing on the overall response. Figure 6(*b*) presents the corresponding results for the dimensionless damping coefficient C_v^p. The C_v^p value exhibits a sharp peak near the first resonant frequency, and much smaller peaks for the higher resonant frequencies. When damping is increased, the peaks become smoother. Similar results have been obtained for higher longitudinal modes *p* and various aspects ratios R/L.

The converged C_a^p values in the region of the dominant frequency are compared in Fig. 7 with those obtained from the simplified formulation (Eq. (72)) as well as with the corresponding values of the equivalent rectangular container (Eq. (*A*8)). The comparison shows a very good agreement between the converged

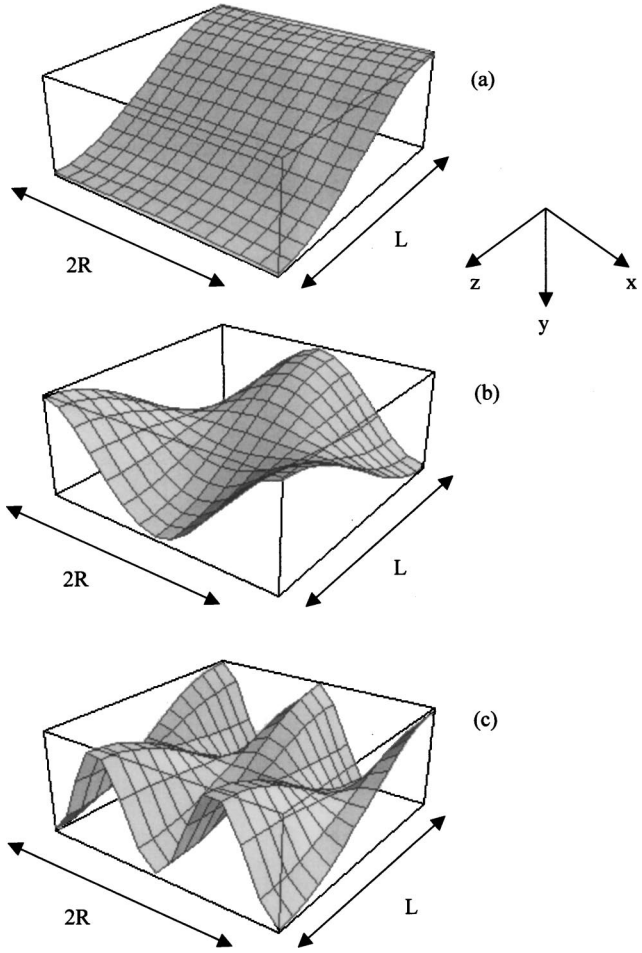

Fig. 5 Eigenmodes in terms of free-surface elevation corresponding to the first three eigenfrequencies ($\omega_1^1, \omega_2^1, \omega_3^1$) of the first longitudinal mode ($p=1$), with $L/R=\pi$

C_a^p values of the horizontal cylinder and the C_a^p values of the equivalent rectangle, whereas the simplified values are reasonably close.

It is possible to demonstrate analytically that for long cylinders ($L\to\infty$), the C_a^p and C_v^p values of a half-full cylinder obtained through the simplified methodology coincide with those of the rectangular "equivalent" container. More specifically, computing the limits of Eqs. (72), (73) and (*A*8), (*A*9) and considering $h=\pi R/4$, one obtains

$$\lim_{R/L\to 0} C_a^p = \lim_{h/L\to 0} [C_a^p]_{\text{rec}} = -\left(\frac{8}{p^2\pi^2}\right)\frac{\lambda^2(1-\lambda^2)}{(1-\lambda^2)^2+(2\xi_p\lambda)^2} \tag{76}$$

and

$$\lim_{R/L\to 0} C_v^p = \lim_{h/L\to 0} [C_v^p]_{\text{rec}} = -\left(\frac{8}{p^2\pi^2}\right)\frac{2\xi_p\lambda^3}{(1-\lambda^2)^2+(2\xi_p\lambda)^2}. \tag{77}$$

5.3 Results for Earthquake Ground Motion. The response of horizontal-cylindrical liquid containers under earthquake excitation is of particular importance for the seismic analysis of pressure vessels used in refineries and petrochemical industries. The efficiency of the proposed methodology to handle an arbitrary type of external excitation is demonstrated calculating the response of a half-full horizontal cylindrical vessel, subjected to the El Centro 1940 seismic ground motion (Fig. 8(*a*)). The vessel has radius $R=1$ m, length $L=12$ m ($L/R=12$), and liquid density $\rho=1000$ kgr/m^3 ($g=9.81$ m/sec^2). According to Eqs. (55) and (60), for this half-full container, the sloshing masses for $p=1$ and $p=3$ are equal to 80% and 8% of the liquid mass M_L, whereas the impulsive mass M_I is equal to 9% of M_L. The linear system of Eqs. (29) is integrated in time ($\Delta t=0.02$ sec) through a fourth-order Runge-Kutta scheme in Matlab programming.

The dependence of the maximum value of the sloshing force $F_{s,\max}$ on the truncation size is presented in Table 1 for zero damping. It is interesting to note that consideration of few terms of the series in the transverse direction (e.g., $n<N=4$) is adequate to provide quite accurate results for engineering purposes. The results are very well compared with those from an equivalent rectangular container. Furthermore, for all longitudinal modes the results from the simplified formulation ($N=0$) are very close to the converged results.

Figures 8(*b*), 8(*c*), and 8(*d*) show the uniform force F_U, the force associated with sloshing F_s and the total force F, respectively for the cylindrical vessel under consideration, under the El Centro earthquake and for 5% damping. The F_s, F values are obtained with a truncation size $N=4$, and for six longitudinal modes ($p<11$), and the maximum total force is 5.87 kN (at 6.83 sec). The results show that sloshing force counteracts the uniform motion force and this is due to the fact that the dominant earthquake excitation frequencies are significantly larger than the dominant sloshing frequencies ω_1^p implies that F_s is out of phase with F_U.

6 Conclusions

A mathematical model is developed for the simple and efficient solution of externally induced liquid sloshing in longitudinal excited half-full horizontal cylindrical containers. The velocity potential is split in two parts, a "uniform motion" potential (trivially obtained) and a potential associated with sloshing. In this configuration, the problem formulation is not separable and the general solution of the sloshing potential is written as a double series expansion of unknown time functions and their associated spatial functions, which are nonorthogonal in the transverse direction. The formulation reduces in a series of systems of linear differential equations (one system for each longitudinal mode), which is truncated and solved numerically. For the particular case of harmonic external source, a series of systems of linear algebraic equations, allowing for a semi-analytical solution. The convergence is generally rapid and a small truncation size N provides very good results.

The sloshing problem is significantly simplified if only the first two terms of the series in the transverse direction ($N=0$) are considered. This simplification yields quite accurate results in terms of sloshing frequencies and forces, especially for containers with relatively large aspect ratio (L/R), and motivates the development of an equivalent mechanical model to approximate the sloshing response of the vessel.

Subsequently, the response of a typical half-full horizontal cylinder subjected to a real seismic event is examined, and the hydrodynamic forces acting on the container are calculated. The results indicate that sloshing has a significant effect on the total force value.

Finally, it is shown numerically and analytically that sloshing frequencies, modes and forces calculated for the half-full horizontal cylinder compare very well with those from an "equivalent" rectangular vessel, especially for long cylinders. Therefore, the "equivalent" rectangle may be used for approximating the half-full horizontal cylinder response for engineering purposes.

Acknowledgments

This work has been partially supported by the Earthquake Planning & Protection Organization (EPPO), Athens, Greece.

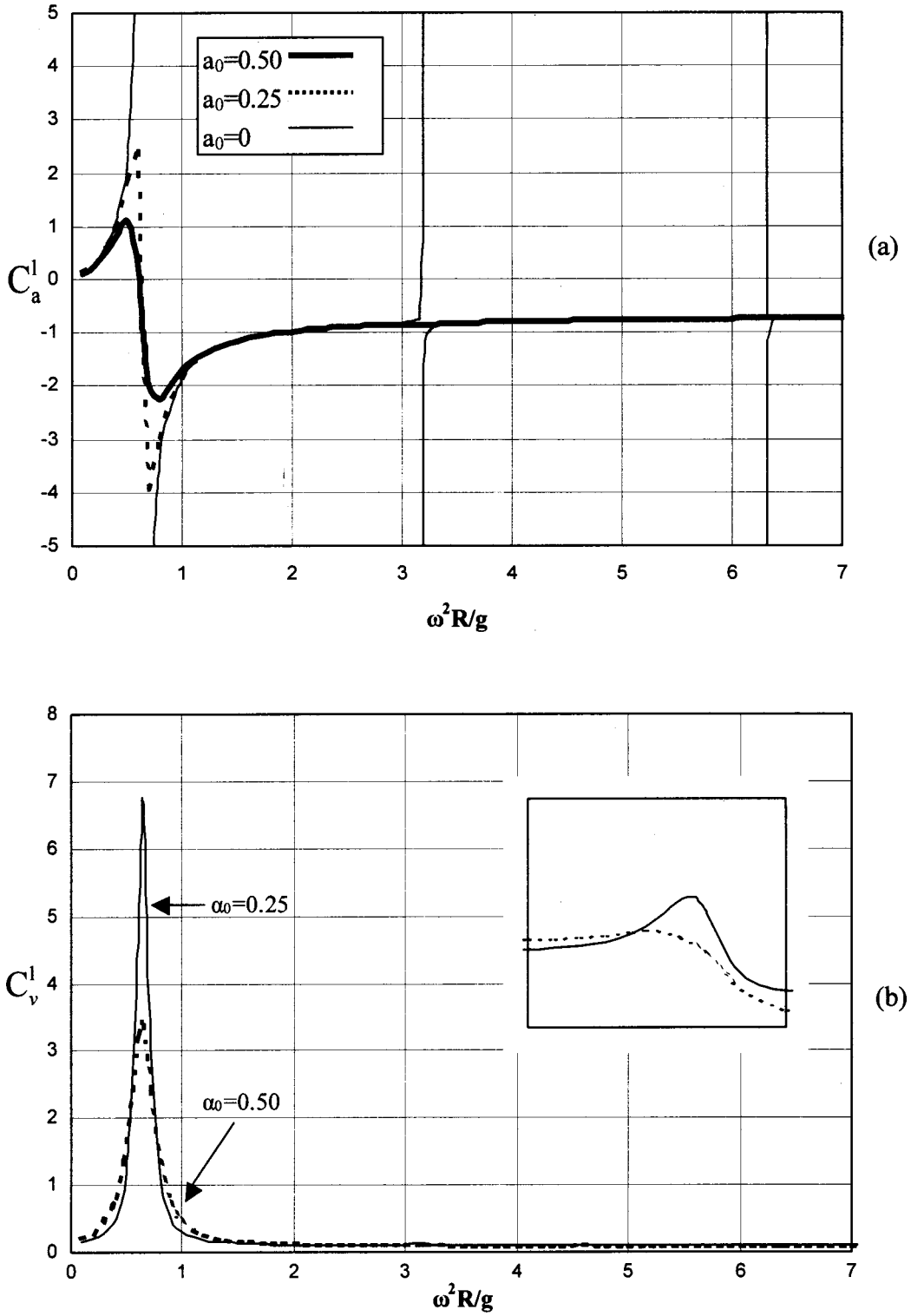

Fig. 6 Converged values of C_a^1 and C_v^1 in terms of external excitation frequency ($\omega^2 R/g$) for $L/R=\pi$, $\alpha_1=0$, and $p=1$

Appendix

Externally Induced Sloshing in Rectangular Containers. The exact analytical solution for the analysis of sloshing in rigid rectangular containers with viscous effects under horizontal excitation has been examined in early works, [3], and is outlined for the sake of completeness. Consider a rectangular container of dimensions $L\times b$ and liquid height h, externally excited in the horizontal z-direction. The total potential Φ satisfies the Laplace equation $\nabla^2\Phi=0$ within the liquid volume, and the following boundary conditions:

$$\frac{\partial\Phi}{\partial z}=\dot{Z}(t), \quad \text{at } z=0 \quad \text{and} \quad z=L \tag{A1}$$

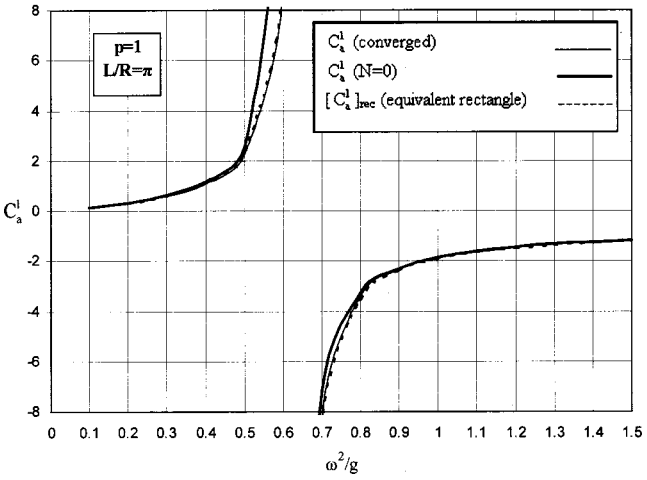

Fig. 7 Added mass coefficient C_a^1 for horizontal cylinder and "equivalent" rectangle

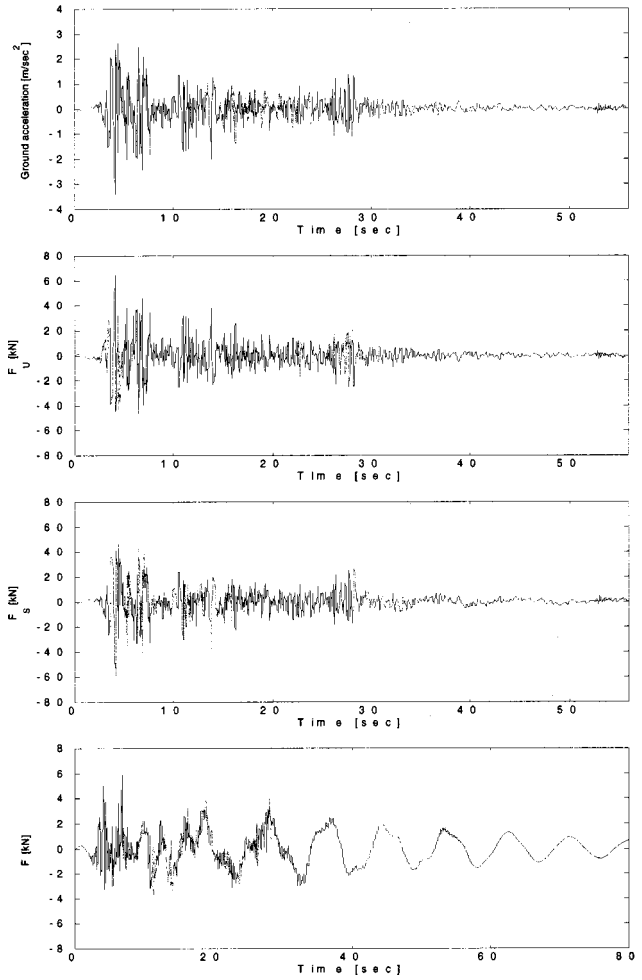

Fig. 8 Response of a half-full cylindrical vessel subjected to the El Centro earthquake in its longitudinal direction for 5% damping. (*a*) El Centro ground motion (source: http://www.vibrationdata.com/elcentro.htm), (*b*) uniform motion force F_U, (*c*) force associated with sloshing F_s and (*d*) total force F.

Table 1 Maximum values of forces associated with sloshing (in kN) for different longitudinal modes—no damping; half-full container ($R=1$ m, $L=12$ m, $g=9.81$ m/sec^2, $\rho=1000$ kgr/m^3)

N	$p=1$	$p<3$	$p<5$	$p<7$	$p<9$	$p<11$
0	51.81	56.26	58.06	58.94	59.50	59.88
1	51.75	56.15	57.91	58.73	59.22	59.51
2	52.10	56.56	58.38	59.28	59.85	60.21
3	51.74	56.13	57.79	58.62	59.12	59.44
4	51.74	56.13	57.86	58.69	59.18	59.35
Equivalent rectangle	51.79	56.22	57.91	58.77	59.28	59.58

$$\frac{\partial \Phi}{\partial y}=0, \quad \text{at } y=0 \tag{A2}$$

$$\frac{\partial^2 \Phi}{\partial t^2}-g\frac{\partial \Phi}{\partial y}=0, \quad \text{at } y=h. \tag{A3}$$

The solution is considered as a sum of an impulsive part $f(z,t)$ given by Eq. (8) and a sloshing part of the following form:

$$\varphi(y,z,t)=\sum_{p=1,3,5}^{\infty} \dot{d}_p \frac{1}{k_p \sinh(k_p h)} \cosh[k_p(y+h)]\cos(k_p z) \tag{A4}$$

where $k_p=p\pi/h$, $p=1,3,5,\ldots$. Equation (A4) is independent of x (transverse coordinate) because of symmetry, and satisfies the Laplace equation, and the kinematic boundary conditions at the tank walls. Enforcing the boundary condition on the free surface, using the orthogonality properties of the trigonometric functions, and introducing a damping term, the following set of uncoupled equations of motion is obtained:

$$\ddot{d}_p+2\xi_p\omega_{\text{rec}}^p\dot{d}_p+(\omega_{\text{rec}}^p)^2 d_p=-\beta_p\ddot{Z} \quad p=1,3,5,\ldots \tag{A5}$$

where

$$(\omega_{\text{rec}}^p)^2=k_p g \tanh(k_p h) \tag{A6}$$

and

$$\beta_p=\frac{4}{p\pi}\tanh(k_p h). \tag{A7}$$

If $Z(t)$ is harmonic (see Eq. (62)), a closed-form expression can be obtained for the unkown time functions $d_p(t)$ and for the flow potential $\varphi(y,z,t)$. In such a case, the dimensionless added mass and damping coefficients become

$$[C_a^p]_{\text{rec}}=-\frac{8L}{h}\left[\frac{1}{(p\pi)^3}\tanh(k_p h)\right]\frac{\lambda^2(1-\lambda^2)}{(1-\lambda^2)^2+(2\xi_p\lambda)^2} \tag{A8}$$

and

$$[C_\nu^p]_{\text{rec}}=-\frac{8L}{h}\left[\frac{1}{(p\pi)^3}\tanh(k_p h)\right]\frac{2\xi_p\lambda^3}{(1-\lambda^2)^2+(2\xi_p\lambda)^2}, \tag{A9}$$

respectively, where $\lambda=\omega/\omega_{\text{rec}}^p$ and ω is the excitation frequency.

References

[1] Currie, I. G., 1974, *Fundamentals Mechanics of Fluids*, McGraw-Hill, New York, Chap. 6.

[2] Miles, J. W., 1956, "On the Sloshing of Liquid in a Cylindrical Tank," *Report No. AM6-5, The Ramo-Woodridge Corp., Guided Missile Research Div.*, GM-TR-18.

[3] Abramson, H. N., 1966, "The Dynamic Behavior of Liquids in Moving Containers," *Southwest Research Institute*, NASA SP-106, Washington, DC.

[4] Housner, G. W., 1957, "Dynamic Pressures on Accelerated Fluid Containers," Bull. Seismol. Soc. Am., **47**, pp. 15–35.

[5] Veletsos, A. S., and Yang, J. Y., 1977, "Earthquake Response of Liquid Stor-

age Tanks,'' *2nd Engineering Mechanics Conference*, ASCE, Raleigh, NC, pp. 1–24.
[6] Haroun, M. A., and Housner, G. W., 1981, ''Earthquake Response of Deformable Liquid Storage Tanks,'' ASME J. Appl. Mech., **48**, pp. 411–417.
[7] Rammerstorfer, F. G., Fisher, F. D., and Scharf, K., 1990, ''Storage Tanks Under Earthquake Loading,'' Appl. Mech. Rev., **43**(11), pp. 261–283.
[8] Veletsos, A. S., and Tang, Y., 1990, ''Soil-Structure Interaction Effects for Laterally Excited Liquid Storage Tanks,'' Earthquake Eng. Struct. Dyn., **19**, pp. 473–496.
[9] Ibrahim, R. A., Pilipchuk, V. N., and Ikeda, T., 2001, ''Recent Advances in Liquid Sloshing Dynamics,'' Appl. Mech. Rev., **54**(2), pp. 133–177.
[10] Moiseev, N. N., and Petrov, A. A., 1966, ''The Calculation of Free Oscillations of a Liquid in a Motionless Container,'' Adv. Appl. Mech., **9**, pp. 91–154.
[11] Fox, D. W., and Kutler, J. R., 1981, ''Upper and Lower Bounds for Sloshing Frequencies by Intermediate Problems,'' J. Appl. Math. Phys., **32**, pp. 667–682.
[12] Fox, D. W., and Kutler, J. R., 1983, ''Sloshing Frequencies,'' J. Appl. Math. Phys., **34**, pp. 669–696.
[13] McIver, P., 1989, ''Sloshing Frequencies for Cylindrical and Spherical Containers Filled to an Arbitrary Depth,'' J. Fluid Mech., **201**, pp. 243–257.
[14] McIver, P., and McIver, M., 1993, ''Sloshing Frequencies of Longitudinal Modes for a Liquid Contained in a Trough,'' J. Fluid Mech., **252**, pp. 525–541.
[15] McCarthy, J. L., and Stephens, D., 1960, ''Investigation of the Natural Frequencies of Fluids in Spherical and Cylindrical Tanks,'' *Report* NASA TN D-252.
[16] Kana, D. D., 1979, ''Liquid Slosh Response in Horizontal Cylindrical Tank Under Seismic Excitation,'' *Southwest Research Institute Report*, Project 02-9238, San Antonio, TX.
[17] Budiansky, B., 1960, ''Sloshing of Liquids in Circular Canals and Spherical Tanks,'' J. Aerosp. Sci., **27**, pp. 161–173.
[18] Kobayashi, N., Mieda, T., Shibata, H., and Shinozaki, Y., 1989, ''A Study of the Liquid Slosh Response in Horizontal Cylindrical Tanks,'' ASME J. Pressure Vessel Technol., **111**, pp. 32–38.
[19] Evans, D. V., and Linton, C. M., 1993, ''Sloshing Frequencies,'' Q. J. Mech. Appl. Math., **46**, pp. 71–87.
[20] Abramowitz, M., and Stegun, I., 1972, *Handbook of Mathematical Functions*, 10th Ed., Dover, New York.
[21] Faltinsen, O. M., 1978, ''A Numerical Nonlinear Method of Sloshing in Tanks With Two-Dimensional Flow,'' J. Ship Res., **22**, pp. 193–202.
[22] Isaacson, M., and Subbiach, K., 1991, ''Earthquake-Induced Sloshing in a Rigid Circular Tank,'' Can. J. Civ. Eng., **18**, pp. 904–915.